Visual Neuroscience (2004), **21**, 913–924. Printed in the USA.

DOI: 10.1017/S095252380421611X

Postsynaptic calcium feedback between rods and rod bipolar cells in the mouse retina

AMY BERNTSON,[1] ROBERT G. SMITH,[2] AND W. ROWLAND TAYLOR[1,3]

[1]John Curtin School of Medical Research and Centre for Visual Sciences, Australian National University, Canberra, Australia
[2]Department of Neuroscience, University of Pennsylvania, Philadelphia
[3]Neurological Sciences Institute, Oregon Health and Sciences University, Beaverton

(RECEIVED January 6, 2004; ACCEPTED September 28, 2004)

Abstract

Light-evoked currents were recorded from rod bipolar cells in a dark-adapted mouse retinal slice preparation. Low-intensity light steps evoked a sustained inward current. Saturating light steps evoked an inward current with an initial peak that inactivated, with a time constant of about 60–70 ms, to a steady plateau level that was maintained for the duration of the step. The inactivation was strongest at hyperpolarized potentials, and absent at positive potentials. Inactivation was mediated by an increase in the intracellular calcium concentration, as it was abolished in cells dialyzed with 10 mM BAPTA, but was present in cells dialyzed with 1 mM EGTA. Moreover, responses to brief flashes of light were broader in the presence of intracellular BAPTA indicating that the calcium feedback actively shapes the time course of the light responses. Recovery from inactivation observed for paired-pulse stimuli occurred with a time constant of about 375 ms. Calcium feedback could act to increase the dynamic range of the bipolar cells, and to reduce variability in the amplitude and duration of the single-photon signal. This may be important for nonlinear processing at downstream sites of convergence from rod bipolar cells to AII amacrine cells. A model in which intracellular calcium rapidly binds to the light-gated channel and reduces the conductance can account for the results.

Keywords: Calcium feedback, Metabotropic synapse, Retinal neurons, Rod bipolar cell, Scotopic signals, Visual system

Introduction

The first synaptic connection in the vertebrate retina is glutamatergic and occurs between the photoreceptors and the bipolar cells (reviewed in Sharpe & Stockman, 1999; Bloomfield & Dacheux, 2001). All photoreceptors produce a common signal—they reduce the release of glutamate from the synaptic terminal when the outer segment is illuminated. However, this signal produces divergent responses in the bipolar cells, which are classified as On- and Off-types by the sign of their response to illumination—light depolarizes On-cells and hyperpolarizes Off-cells. These different responses, to the common glutamatergic input, are due to different postsynaptic glutamate receptors. The dendritic tips of On-bipolar cells express metabotropic glutamate receptors, designated as mGluR6 (Slaughter & Miller, 1981; Masu et al., 1995; Vardi et al., 2000). In the dark, the glutamate released by photoreceptors initiates a biochemical cascade mediated by $G_{\alpha o}$ (Vardi, 1998; Nawy, 1999; Dhingra et al., 2000, 2002) which ultimately closes cation channels (Wilson et al., 1987; Nawy & Jahr, 1990; Shiells & Falk, 1990; Yamashita & Wässle, 1991; Shiells & Falk, 1992*b*). During a light stimulus, when glutamate release from the photoreceptors is suppressed, the cation channels open and generate a depolarizing current carried by sodium, potassium, and calcium ions.

Under scotopic conditions (starlight–moonlight), the major pathway for signals from rod photoreceptors is through a single class of bipolar cell, the rod bipolar cell (Dacheux & Raviola, 1986; Wässle et al., 1991; Yamashita & Wässle, 1991). Similar to cone bipolar cells (CBCs), rod bipolar cells (RBCs) express mGluR6 receptors, and are depolarized by light stimuli (Dacheux & Raviola, 1986; Berntson & Taylor, 2000; Euler & Masland, 2000). Other pathways for rod signals exist, through gap junctions between rods and cones at mesopic backgrounds (Nelson, 1977; Kolb & Nelson, 1983; Smith et al., 1986), or alternatively through chemical synapses directly onto some classes of off-CBC (DeVries & Baylor, 1995; Soucy et al., 1998)

The rod pathway *via* RBCs to ganglion cells comprises several stages of anatomical convergence. Each RBC collects signals from 20–50 rods, and about 25 RBCs converge onto each AII amacrine, the next neuron in the rod pathway (Sterling et al., 1988; Strettoi et al., 1990; Vaney et al., 1991; Strettoi et al., 1992; Tsukamoto et al., 2001) At low light levels, the rod signal in the ganglion cell consists of single-photon signals (Barlow et al., 1971; Mastronarde, 1983) which are transmitted as independent events at each relay within the rod pathway. At the major points of conver-

Address correspondence and reprint requests to: W. Rowland Taylor, Neurological Sciences Institute, Oregon Health and Science University—West Campus, 505 NW 185th Avenue, Beaverton, OR 97006, USA. E-mail: taylorw@ohsu.edu

gence, from rods to RBCs and from RBCs to AIIs, the increased noise level due to convergence would be expected to overwhelm the signal-to-noise (S/N) ratio of the single-photon events if the synapse were linear (Baylor et al., 1984; Smith & Vardi, 1995; van Rossum & Smith, 1998). Therefore if the single-photon signals are to be resolved at these synapses, temporal filtering and nonlinear processing are essential (van Rossum & Smith, 1998).

Recently, we have shown that despite having similar postsynaptic receptors, On-CBC and RBC synapses have a qualitative difference in their signal transfer. During a saturating light step the response in the On-CBCs is often sustained, whereas the RBCs produce an initial transient component followed by rapid inactivation to a maintained plateau (Berntson & Taylor, 2000). We show here that the inactivation observed for the synapses with rod photoreceptors is similar to a much slower calcium-dependent inactivation reported for dog-fish and salamander bipolar cells (Shiells & Falk, 1999; Nawy, 2000; Snellman & Nawy, 2002). We propose that the calcium feedback might be important for transmission of single-photon signals.

Materials and methods

Preparation and recording

Retinas were isolated from dark-adapted Black6 mice 4–6 weeks of age in accordance with institutional guidelines monitored by the Animal Experimentation Ethics Committee at the Australian National University. The animals were killed with a lethal intraperitoneal injection of Nembutal (0.1 ml, 100 mg/ml) and the eyes immediately enucleated and placed in oxygenated Ames' medium at room temperature. Vertical sections, 200 μm thick, were prepared as described previously (Berntson & Taylor, 2000). All procedures were performed under infrared (>850 nm) illumination. Whole-cell patch-clamp recordings were made from 37 rod bipolar cells. Initially, the RBCs were identified from the morphology revealed by lucifer-yellow fills. In later experiments, they were identified based upon the position of the soma, the sensitivity to light, and the presence of marked, intensity-dependent inactivation as shown below. Cells were held at −50 mV.

Patch electrodes, fabricated from borosilicate glass, had a resistance of 10–15 MΩ and were coated with Sylgard® (Dow Corning, MI) before use. The electrode was connected to a HEKA EPC-9 amplifier (Heka Elektronic, Lambrecht/Pfalz) *via* a Ag/AgCl junction. The recording chamber was grounded through a Ag/AgCl reference electrode. During recordings, current signals were filtered at 2.5 kHz (8-pole Bessel filter) and sampled at 5 kHz. Further digital filtering of the signal was performed prior to analysis using the "smooth" operation in Igor (WaveMetrics, Lake Oswego, OR). This implements a low-pass filter with a Gaussian impulse response. The effective −3 dB frequency was set to ~60 Hz.

Solutions

Recording electrodes were filled with one of three intracellular solutions. The "control" intracellular solution contained cesium as the main cation, and included 1 mM of the calcium chelator, ethylene glycol-bis(β-aminoethyl ether)-N,N,N′,N′-tetraacetic acid (EGTA). The "BAPTA" intracellular solution was identical to the control, except that 10 mM 1,2-bis(2-aminophenoxy)-ethane-N,N,N′,N′-tetraacetic acid (BAPTA) replaced the 1 mM EGTA. Finally, a "zero calcium buffer" solution contained potassium as the main cation and no calcium chelator. Potassium was used in place of cesium so that current-clamp recordings could be made, but current-clamp data is not presented here.

A complete listing of the control and zero-calcium-buffer solutions follows. Control solution (in mM): 110 Cs-gluconate, 5 CsCl, 5 NaCl, 1 EGTA, 0.1 $MgCl_2$, 5 Na-HEPES, 5 Na-ATP, and 0.5 Na-GTP. Zero-calcium-buffer solution (in mM): 112 K-gluconate, 5 NaCl, 5 KCl, 0.1 $MgCl_2$, 5 Na-HEPES, 5 Na-ATP, and 5 Na-GTP. Intracellular solutions were adjusted to pH 7.4 with the appropriate hydroxide.

The recording chamber containing the slices was continuously perfused at 2–3 ml/min with Ames medium (Sigma Chemical Co., St. Louis, MO), heated to 35°C, and equilibrated with 95% O_2/5% CO_2 (pH 7.45).

Light stimulus

The retina was stimulated with the green phosphor of the Apple Multiple Scan 15AV monitor (75-Hz frame rate), which has a single peak at 540 nm with a half-width of 75 nm. All stimuli illuminated the whole slice. Stimulus "flashes" comprised a single frame lasting less than 1 ms at any one point on the screen, while "steps" consisted of multiple consecutive frames. The light stimuli were focused onto the preparation through the 40×/0.8NA microscope objective. The orientation of the slices beneath the objective was such that the light was incident upon the photoreceptors approximately normal to the long axis of the outer segments. Light intensities were measured at the preparation and converted to photoisomerizations per rod (Rh*/rod), using a collecting area of 0.5 μm^2 reported for mouse rods in the slice preparation (Field & Rieke, 2002*a*). For light steps, we specified intensities as Rh*/rod/rod-integration time, where rod integration time, T_{rod}, was set to 0.2 s (Penn & Hagins, 1972; Baylor et al., 1984). The light output of the computer monitor was linearized using a lookup table. Twelve fixed intensity levels were used and the relative intensity of each level was measured directly to obviate small errors in the linearization. The twelve intensity levels could be shifted along the intensity axis by up to 2.5 log units using calibrated neutral density filters.

A model for Ca-feedback at the rod synapse

The model constructed to account for the properties of the flash and step responses was similar to that described by van Rossum and Smith (1998), and is summarized in Fig. 9. It consisted of 20 rods connected to a single rod bipolar cell, each at an individual dendritic tip. The voltage responses of the rods were simulated with a model similar to one described by Nikonov et al. (1998), but adjusted to give a single-photon response duration similar to that in mammalian rods (van Rossum & Smith, 1998). The recovery of the model's rod response was similar to real rods except that at flash intensities above 10 R*/rod/T_{rod}, the model did not accurately depict the rod aftereffect, a prolonged slow recovery phase. The model had a faster recovery phase, similar to that for weaker flashes, which reduced the recovery of the RBC currents it produced (Fig. 11) compared to recordings from the real RBCs. This inaccuracy did not impact our main conclusions. The rate of photon absorption explicitly included Poisson fluctuation. The dark resting potential of the rods was set to −40 mV, and the threshold for release of neurotransmitter was set to produce a constant high rate of neurotransmitter release from the terminal in the dark.

Each rod terminal released neurotransmitter at a rate set by an exponential function of the presynaptic rod voltage above a preset threshold (Smith, 1992). For most simulations the exponent was set to 1.6–1.8 / mV (e-fold change in 0.55–0.63 mV), which meant that release changed by about 5–6 fold/mV. This relatively high gain allowed the synapse to pass the signal from one photon but caused it to saturate at two photons. This assumption was necessary to allow the synapse from one rod to signal a single-photon signal with an adequate *S*/*N* ratio at a plausible synaptic release rate of 100 vesicles/s (van Rossum & Smith, 1998). However, neither vesicle fluctuation noise nor dark continuous noise were included in the model. The released neurotransmitter transient was filtered with a second-order low-pass filter (each stage 4 ms) and bound to the simulated mGluR6 receptor with a saturation function having a Hill coefficient of 2. The simulated mGluR6 receptor controlled a postsynaptic second-messenger signaling cascade with a time course, simulated as a second-order low-pass filter. The time constant of each stage was 20 ms. The impulse response of the signaling cascade had a smooth rise and fall and a ~40 ms time constant, similar to the time delays seen in the RBC response to nonsaturating flashes of light (Figs. 4 & 6, Robson & Frishman, 1995). Activation of mGluR6 receptors *reduced* the concentration of a second messenger that bound to and opened a nonspecific cation channel. Since the concentration of the second messenger could not go below zero, this produced a sharp threshold in the signal transfer, which was simulated as a static nonlinearity (Shiells & Falk, 1994; van Rossum & Smith, 1998). The level of the nonlinearity was set to about 40% of the amplitude of the single-photon peak response, but for this study the exact level was not critical (van Rossum & Smith, 1998).

The cation channel was simulated with a Markov diagram having six states. It was given an open conductance of ~640 pS (32 channels of 20 pS/channel) to match observed currents and was arbitrarily assigned a permeability for Ca^{2+} of 0.05. The ion channel had two agonist binding sites, and a single binding site for Ca^{2+}, and was simulated in the "macroscopic" mode where occupancy of the states was a fraction of 1 (Fig. 10). The binding and unbinding rates for Ca^{2+} were set to achieve the relatively low plateau currents (~20% of peak), but these rates also lengthened the channel recovery time beyond the realistic range (300–400 ms). To achieve a recovery time in the proper range, it was necessary to add the kinetic rate modifier "A" to increase the kinetic rate for recovery when both the ligand and $[Ca^{2+}]_i$ were low (Kuo & Bean, 1994). Even with this higher rate, the recovery from inactivation was dominated by the single step of calcium unbinding from the channel. At high agonist concentrations (when glutamate receptor occupancy was very low), the channel was either conducting, or if a calcium ion was bound, nonconducting. Therefore the amount of current flowing through the fully liganded channels depended inversely on $[Ca^{2+}]_i$ of the RBC dendritic tip. The model included calcium pumps, which were adjusted to reduce $[Ca^{2+}]_i$ with a time constant of about 100 ms. The absolute values for the Ca^{2+} permeability and the calcium-binding kinetics were not critical because the $[Ca^{2+}]$ affinity of the cation channel's kinetic equations were set to produce the desired binding properties (see Fig. 10). Thus in the model, binding of Ca^{2+} represented a negative feedback that limited the amplitude and duration of the postsynaptic response. The entire model including light stimuli, noise properties, photoreceptor kinetics, synaptic mechanisms, ion channel kinetics, and electrical responses was implemented in the Neuron-C simulation language (Smith, 1992; van Rossum & Smith, 1998). The stimulator is described at, and can be downloaded from http://retina.anatomy.upenn.edu/rob/neuronc.html. The script file for the model is available *via* ftp: ftp://retina.anatomy.upenn.edu/pub/rob/rbc_ca_feedback_ model.

Results

In 37 RBCs, a saturating light step evoked a transient inward current followed by a sustained plateau current (Fig. 1A). The plateau current was maintained for the longest duration steps applied, and was often followed by a small transient outward current at the termination of the light stimulus (Fig. 1B). Light responses in On-CBCs saturated at light intensities about 50-fold higher. Since the light responses were completely abolished by 50 μM APB (data not shown), it seems that the ionotropic glutamate receptors reported to be present on rod bipolar cells (Hack et al., 2001; Kamphuis et al., 2003) do not contribute to the light responses reported here. Although the amplitude of the light-evoked current was comparable in the RBCs and On-CBCs, a transient phase was not observed in the On-CBCs (Fig. 1C). A possible explanation for the transient phase is that light generates

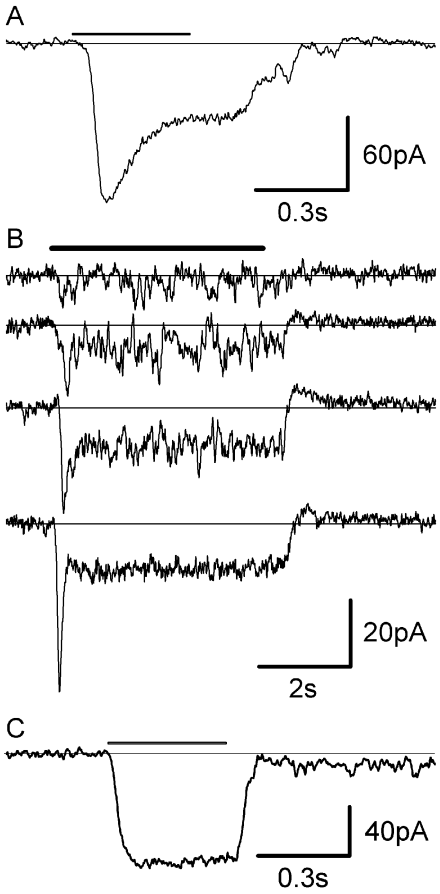

Fig. 1. Only RBCs display inactivation. A: RBC response to saturating light step (~100 Rh*/rod/s) showing the characteristic transient inward current. B: Responses in RBCs recorded at light intensities that covered the dynamic range of the cell (top to bottom: 0.1, 0.3, 1.6, & 13 Rh*/rod/s). At high intensities, a transient phase preceded a sustained inward current that lasted for the duration of the light step. C: On-CBCs produced sustained currents during saturating light steps (equivalent to $\sim 4 \times 10^4$ photons/μm^2/s at a wavelength of 500 nm).

a delayed outward inhibitory current in the RBCs. To test this hypothesis, we measured step responses at a range of membrane potentials.

Peak and sustained components share a common reversal potential

The membrane potential was stepped to a series of different values and the same saturating light stimulus applied each time. As expected from the data in Fig. 1, the stimulus elicited a transient inward current at negative potentials that quickly decayed to a steady plateau current. At positive potentials, the transient phase largely disappeared and the response became more sustained (Fig. 2A). We measured average current–voltage relations in nine RBCs at two time points, corresponding to the peak and plateau of the light responses (Fig. 2B). At both time points the peak current–voltage relation was linear with a reversal potential of +7 mV, consistent with the activation of a nonselective cation channel. At the later time point, the current–voltage relation became sublinear at hyperpolarized potentials, but the reversal potential was the same. The positive reversal potential indicates that few if any inhibitory inputs were active under these recording conditions. The dependence of response wave shape on the postsynaptic clamp potential suggests that the transient phase of the RBC light response is initiated postsynaptically, and thus we will refer to the transient phase as "inactivation".

Inactivation is due to calcium influx

Previous studies have suggested that calcium ions modulate the amplitude of mGluR6 mediated responses (Yamashita & Wässle, 1991; Shiells & Falk, 1999; Nawy, 2000) and so we asked whether the inactivation was due to calcium influx through the light-gated channels. If calcium influx is involved, then the inactivation should become more pronounced at negative potentials due to the increased driving force for calcium influx. Similarly, inactivation should be reduced or even disappear at positive potentials. Inactivation, measured as the ratio of the plateau current to the peak current, was slightly stronger at −95 mV (0.37 ± 0.09) than at −20 mV (0.55 ± 0.15, $P = 0.0032$, *t*-test, $n = 9$, Fig. 2C). Over the same voltage range, the time constant for inactivation averaged 63 ± 6 ms (range 56–71 ms) but was essentially voltage independent (Fig. 2D). It was not possible to measure the degree or rate of inactivation between −20 and +20 mV because the responses close to the synaptic reversal potential were too small, however, positive to +20 mV the inactivation was much reduced consistent with a lower influx of calcium due to the reduced electrical driving force.

To test the calcium hypothesis directly, we included the fast calcium chelator BAPTA in the recording electrode. In some cases, upon breaking into the cell with a BAPTA-filled recording electrode, the light-evoked response displayed inactivation (Fig. 3A) but tens of seconds later, the inactivation was strongly suppressed, and the peak current was larger (lower traces, Fig. 3A). Usually the BAPTA effect occurred much more rapidly, and the inactivation was already abolished at the first light stimulus without observing an increase in the peak current (Fig. 3B). Diffusion of BAPTA into the soma and dendrites is expected to be very rapid due to the very small size of the cells. Consistent with the calcium hypothesis, the intracellular BAPTA also eliminated the voltage dependence of the RBC light response waveform (Fig. 3C), resulting in almost identical peak and plateau current–voltage relations (Fig. 3D). The

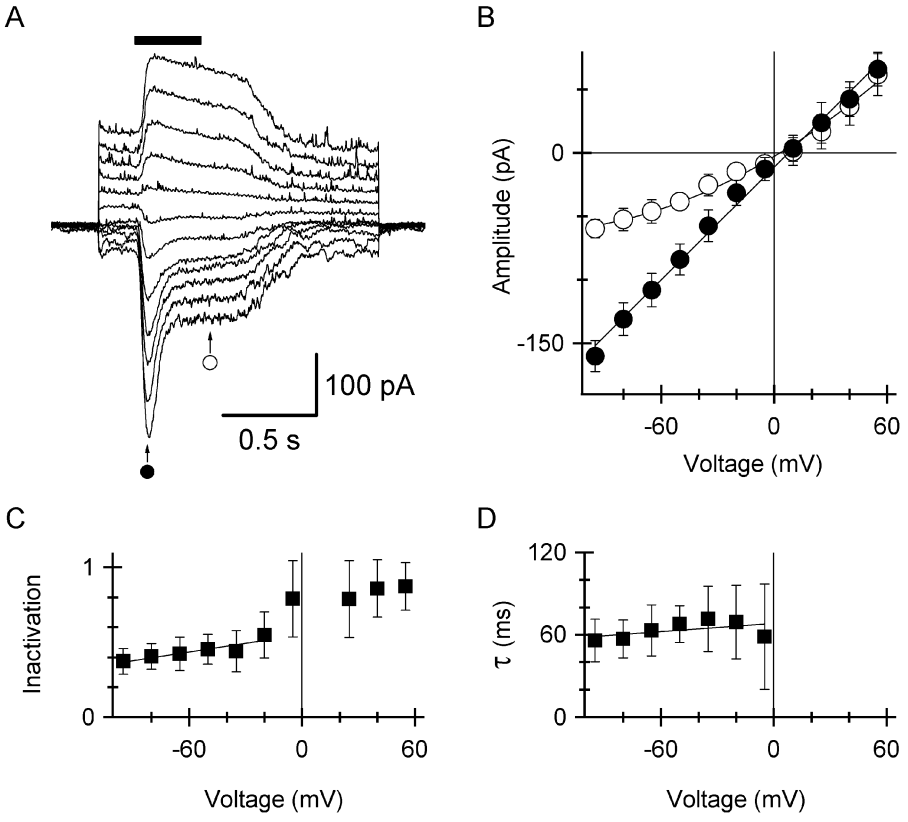

Fig. 2. Inactivation disappears at positive holding potentials. A: Responses to saturating steps of light (~100 Rh*/rod/s) applied at a series of holding potentials (−90 to +45 mV by 15-mV increments). The symbols show the time points used to measure the current–voltage relations in *B*. B: Average peak and plateau current–voltage relations from nine cells at the time points indicated in *A* The line fitted to the peak responses has a slope of 1.5 nS, and intersects the voltage axis at +7 mV. C: Ratio of the plateau current to the peak current plotted against holding potential. D: Inactivation time constant plotted against holding potential.

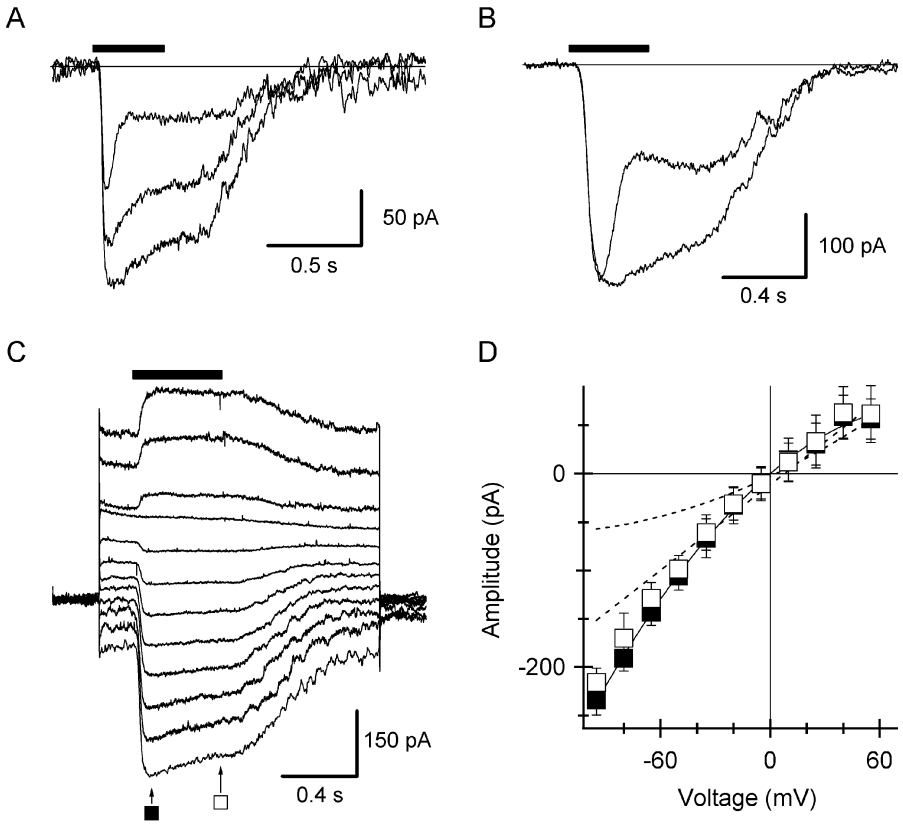

Fig. 3. Intracellular BAPTA suppresses inactivation. A: Records obtained during equilibration of the BAPTA with the intracellular milieu. The top trace was recorded upon break-in, and the lower traces were obtained 25 s and 38 s later. B: The top trace shows the response upon break-in, while the second response was obtained only 3 s later. BAPTA suppression of the feedback was complete at this time. Some cells showed an increase in the peak current (*A*), while in others it was unchanged (*B*). C: Responses to saturating steps of light at a series of holding potentials (as in Fig. 2A) in the presence of intracellular BAPTA. D: Average current–voltage relations in five cells in the presence of intracellular BAPTA. Current-voltage relations were measured at two time points as in Fig. 2B. The smooth line through the points shows a second-order polynomial with coefficients −0.007 pA, 1.6 pA/mV, and −9.18 pA/mV^2. The broken lines show the control *IV* relations from Fig. 2A for comparison. Light intensities: *A* ~100 Rh*/rod/s, *B* ~220 Rh*/rod/s, *C* ~220 Rh*/rod/s.

slight inward rectification of the current–voltage relations recorded with BAPTA was not observed for the peak current–voltage relation in the controls (dotted lines from Fig. 2B). The results indicate that the inactivation is mediated by an increase in intracellular calcium concentration.

Inactivation is stronger at high light intensities

If the calcium-dependent inactivation is caused by the light-evoked current, the inactivation should depend on the size of the postsynaptic current and thus on the stimulus intensity. RBC intensity–response relations were measured using three intracellular solutions (Fig. 4). A control solution contained 1 mM EGTA, a second, potassium-based solution did not include EGTA (no calcium buffer), and a third cesium-based solution contained 10 mM BAPTA rather that EGTA as the calcium buffer. At lower intensities, the responses looked sustained for the duration of the light step because the noise peaks did not vary systematically during the response, while at higher intensities inactivation of the inward current is seen (Fig. 4A). The intracellular solution contained no calcium buffer during this recording, but responses during recordings using the solution containing 1 mM EGTA were indistinguishable. As expected from the previous results, 10 mM intracellular BAPTA abolished inactivation (Fig. 4B).

The intensity–response relations shown in Fig. 4C were described by the function,

$$I = I_{\max} L^h/(L^h + L_{1/2}^h), \quad (1)$$

where L is the light intensity, I_{max} is the saturated response amplitude, $L_{1/2}$ is the half-maximal light intensity, and h is an exponent referred to as the Hill coefficient. Average values for h and $L_{1/2}$ (± 1 standard deviation) calculated from the fits to individual cells in the three groups are listed in Table 1. The difference in the Hill coefficient for the step intensity–response relations in control and zero-buffer conditions was not statistically significant, but was similar to that observed for mammalian rod photoreceptors (Schneeweis & Schnapf, 1995). However, in the presence of BAPTA, the step intensity–response relation was steeper than in control and no-buffer conditions ($P < 0.0001$).

The ratio of the plateau current amplitude to the peak current amplitude showed a consistent downward trend as a function of light intensity (Fig. 5A). At the lower intensities the amplitude of the plateau current was ~50% that of the peak, while at higher intensities (even well below saturation) it was stable at ~20%. Thus, inactivation became more marked at higher intensities. It is noteworthy that the stronger inactivation was not due to a continual decrease in the plateau current level with increasing intensity (see Fig. 4A). Rather, the plateau current became stable at subsaturating intensities, and the decrease in the amplitude ratio was due to the peak response becoming relatively larger at higher intensities The invariant plateau level is paralleled by the inactivation time constant measured by fitting an exponential function to the decay phase of the responses. The average inactivation time constant was 64± 7 ms ($n = 6$) in control (Fig. 5B, circles) and 71 ± 5 ms ($n = 9$) with the no calcium buffer solution (Fig. 5B, squares). The inactivation time constants suggest that the calcium-dependent inactivation may occur rapidly enough to affect the time course of the flash response. Therefore, we decided to test the effect of the fast calcium chelator BAPTA on the flash response.

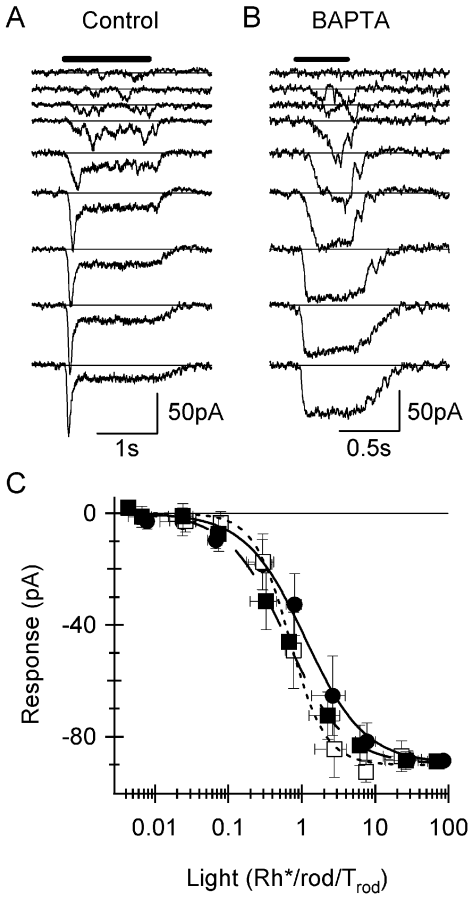

Fig. 4. Inactivation is intensity dependent. A: Responses to 1.5-s light steps of increasing intensity become more transient with increasing intensity. B: Inactivation is abolished at all intensities with intracellular BAPTA. C: Intensity–response relations measured from the peak light responses in control (●), zero-buffer (■), and BAPTA (□). The smooth curves were the best fits of eqn. (1), and the parameters are shown in the Table 1. The records in *A* and *B* correspond to light intensities 0.01, 0.02, 0.07, 0.3, 0.8, 2.6, 7.7, 28, and 85 Rh*/rod/T_{rod}.

Calcium feedback shapes the flash response

Intracellular BAPTA broadened the flash responses recorded in RBCs. The width at half-height of the flash response in control conditions (Fig. 6A) was 136 ± 25 ms (n = 6) but was 250 ± 21 ms (n = 5) in the presence of BAPTA (Fig. 6B) ($P < 0.0001$), an increase of 180%. Thus, calcium plays an active role in turning off the RBC flash response. Although BAPTA might have caused a slight increase in the Hill coefficient estimated from the intensity–response relations for step responses, the same was not evident for flash responses (Fig. 6C, Table 1). Like the half-width measurement, the time-to-peak of the flash responses was smaller in control, but to a lesser degree, and only at the highest intensities (Fig. 6D) suggesting that the calcium feedback might not be rapid enough to strongly shorten the activation phase, except where a flash of more than 1 photon would elicit a faster rise time. In some cases the calcium feedback effectively limited the amplitude of the initial transient and plateau phases (Fig. 3A), but due to the variable rate at which the BAPTA diffused in and the responses washed out (Figs. 3A & 3B), it is not possible to provide a quantitative analysis of the effects on the amplitude. However, the

Table 1. *The effects of different calcium buffering conditions on the Hill coefficients and half-maximal light intensities recorded from rod bipolar cells*[a]

Condition	N	h (Hill coefficient)	$L_{1/2}$ (Rh*/rod/T_{rod})
Step: Zero-buffer	9	1.10 ± 0.04	0.61 ± 0.02
Step: Control (EGTA)	8	1.07 ± 0.11	1.11 ± 0.12
Step: BAPTA	6	1.78 ± 0.16	0.68 ± 0.04
			$L_{1/2}$ (Rh*/rod)
Flash: Control (EGTA)	7	1.43 ± 0.12	0.75 ± 0.05
Flash: BAPTA	6	1.53 ± 0.15	0.54 ± 0.10

[a]N indicates the number of cells used to generate the average intensity–response relations. T_{rod} = 0.2 s. The errors in the parameter estimates were obtained from the fitting routine.

flash experiments show that the calcium feedback is rapid and persistent enough to generate inactivation for stimuli shorter than the integration time of the postsynaptic response. The lack of inactivation observed during low intensity step stimuli (Fig. 1B, upper records) may be due to the low effective frequency of stimulation. At low intensities, the random capture of photons by the connected rods is infrequent, so that enough time elapses

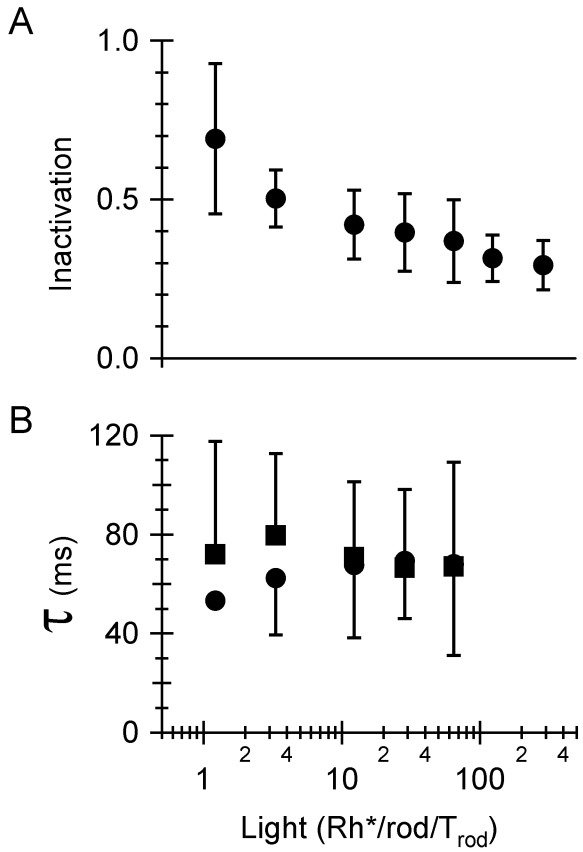

Fig. 5. Dependence of inactivation on stimulus intensity. A: The fractional inactivation, calculated as for Fig. 2C, was more pronounced at higher intensities (●). B: Average decay time constants from 14 cells, in control (●), and no-EGTA intracellular solutions (■) were independent of the stimulus intensity.

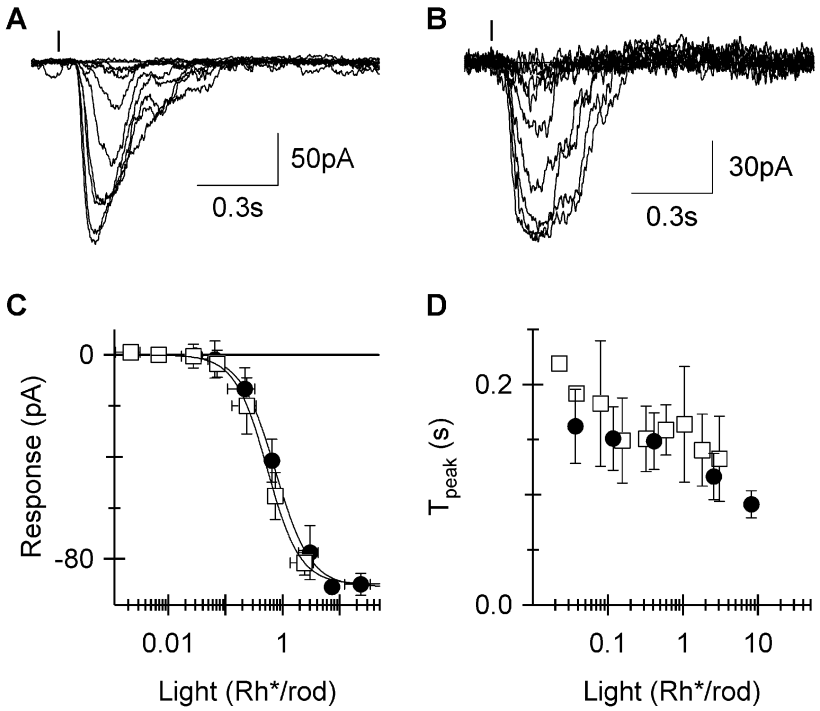

Fig. 6. Calcium feedback shapes the flash response. The vertical marks show the timing of the flash stimuli in *A* and *B*. Flash responses in control (*A*) and with the BAPTA intracellular solution (*B*) were recorded over a range of intensities from threshold to saturation (0.02, 0.04, 0.08, 0.16, 0.33, 0.61, 1.1, 1.9, and 3.2 Rh*/rod). C: Flash intensity–response relations in control (●, n = 9), and BAPTA (□, n = 6). D: The time to peak of the flash responses decreased slightly with increasing intensity, especially for the control responses (Control ●, n = 9 and BAPTA □, n = 6).

between these events for the postsynaptic machinery to recover from inactivation. The experiment in Fig. 7 tests this notion. A series of eight identical flashes are presented at increasing frequencies. At a subsaturating intensity, the response to the first flash is only slightly larger than subsequent responses (Fig. 7A), while for the saturating stimulus, the first response produces considerable inactivation of the subsequent responses (Fig. 7B). Thus, increased intensity alone is sufficient to produce inactivation. It is also evident that increasing the stimulus frequency produced more inactivation, since the amplitudes of the individual flash responses became progressively smaller (1st to 3rd rows in Fig. 7). Thus, at lower frequencies there is more time for the cell to recover between flashes. The next series of experiments was designed to ascertain how quickly recovery occurred.

How fast is the recovery from inactivation?

Recovery from inactivation was assessed using a two-flash protocol. Each stimulus trial comprised a conditioning flash followed at a variable time by an identical test flash. The time between stimulus trials was 5 s. The amplitude of the test flash response relative to the conditioning flash response was used to monitor recovery. When the flashes were separated by 200 ms, the amplitude of the second flash response was suppressed to about 40% compared to the first (top trace, Fig. 8A). In subsequent trials, as the delay between the flashes was increased, the response to the second flash grew larger until it reached a constant amplitude. In five cells, the second flash response recovered with an exponential time constant of 375 ms (Fig. 8C).

The identical experiment was performed in the presence of intracellular BAPTA (Fig. 8B). For the shortest delay between the

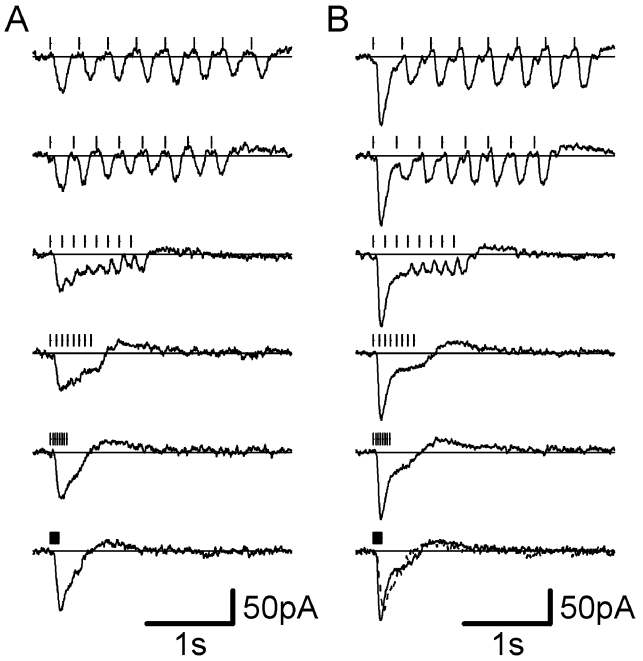

Fig. 7. Inactivation is both intensity and frequency dependent. A: At a subsaturating intensity, the first response of the series is only slightly larger than subsequent responses. B: At a saturating intensity, the first flash is enough to generate significant inactivation. Each record is the average of four (*A*) or three (*B*) individual responses. The bottom record in *A* has been superimposed on *B* for comparison (dotted line). The half-saturating intensity for this cell was ~0.7 Rh*/rod. Flash intensities were ~0.8 Rh*/rod for *A* and ~4.5 Rh*/rod for *B*.

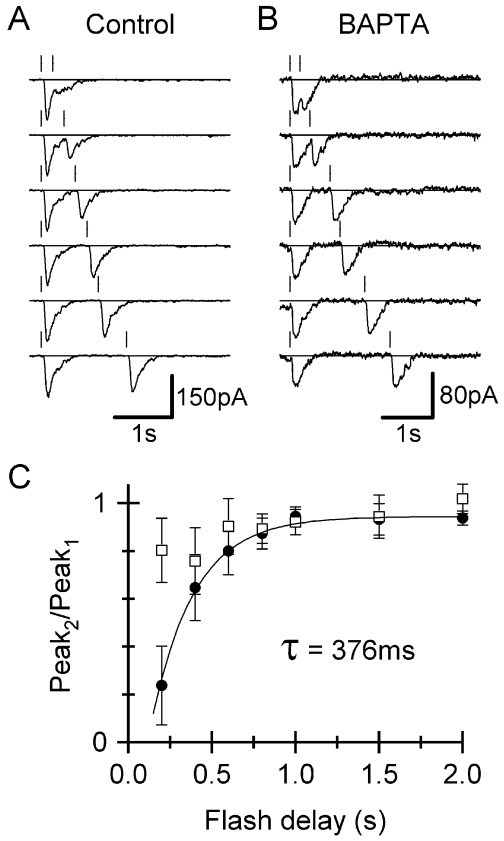

Fig. 8. Recovery from inactivation occurs in a fraction of a second. A, B: The vertical marks show the timing of the identical flash stimuli. Inactivation induced by the first (conditioning) flash is measured as a reduction in the amplitude of the second, test flash. With intracellular BAPTA, inactivation is blocked and the amplitude of the second flash is unaffected by the conditioning flash. Flash intensity ~4.5 Rh*/rod. C: The relative amplitude of the second flash, plotted against delay between the flashes, monitors the recovery from the inactivation induced by the conditioning flash. The solid line shows that recovery is approximately exponential with a time constant of 375 ms. The open squares show average results with intracellular BAPTA.

flashes (200 ms), the response to the second flash was very close in amplitude to that of the first flash. Subsequent stimulus trials show that the amplitude of the second flash response in the presence of BAPTA is independent of the delay between the two flashes (Fig. 8B). This result supports the hypothesis that the suppression of the test flash response in control conditions is due to a rise in postsynaptic calcium concentration.

Results from a model of calcium feedback

The influx of calcium could interrupt signaling between the mGluR6 receptors and the effector cation channel at several different sites. To provide some insight about the calcium feedback mechanism, we developed a model that included realistic simulations of the photoresponses, synaptic binding and saturation, a second-messenger whose activity was reduced by the activated postsynaptic receptor, and a ligand-gated cation channel (Fig. 9). Most of the model's components were taken from a previous model (van Rossum & Smith, 1998), but we added calcium feedback inhibiting the channel. In the present model, the Ca^{2+} ions bound directly to the channel and reduced its conductance (Fig. 10; see Nawy, 2004). The model included 20 rods each providing a synaptic connection to the rod bipolar cell at a separate dendritic tip.

We adjusted the model parameters to reproduce the maximum current and time-to-peak of the step responses recorded from RBCs (Fig. 11A). The relative amplitude of the plateau phase also matched that observed, and was determined in the model by adjusting the affinity of Ca^{2+} for the channel. At low intensities, the step response was sustained due to the low rate at which photons elicited responses in the connected rods. At higher intensities, most of the connected rods were activated simultaneously, and once activated, the calcium channels were converted to the low-conductance state. In agreement with the experimental results, the model produced a transient phase, with a decay phase similar to the time course of the flash response. As expected, addition of intracellular BAPTA to the model blocked the effects of the calcium influx (Fig. 11B). The model also reproduced the effects of BAPTA on the time course of the flash responses, with a slight increase in the amplitude of the current, as was observed in some cells (Figs. 11C & 11D). The parameter "A" (Fig. 10) allowed setting the recovery from inactivation independently from its affinity for calcium. When recovery from inactivation was set close to that observed experimentally, the model correctly reproduced the responses to trains of flashes (Fig. 12A), and the suppression of the second response during paired-pulse stimuli (Fig. 12B).

Discussion

The results demonstrate that during light-evoked responses, a rise in the intracellular calcium concentration produces rapid negative feedback, which suppresses the light-evoked current. It seems likely that the calcium enters the cell through the same channels activated by the light, since depolarization, which reduces the electrical driving force on calcium influx also reduces the suppression. However, these results do not discount a role for calcium released from intracellular stores. Several previous reports have shown that calcium suppresses the light-evoked responses in bipolar cells of dogfish and salamander (Shiells & Falk, 1999, 2000; Nawy, 2000; Snellman & Nawy, 2002) The present results imply that in mouse the feedback is much faster, occurring within tens of milliseconds rather than seconds, and that recovery is also fast, occurring within a fraction of a second. Thus, the calcium-mediated feedback in mouse has the potential to regulate the sensitivity of the rod to RBC synapse on timescales much shorter than is possible for the feedback reported in lower vertebrates. Indeed, our results show that the duration of the flash response over a range of intensities is limited by calcium feedback.

The current–voltage relations of the photoresponses were linear in control (Fig. 2B), and showed slight inward rectification in the presence of intracellular BAPTA (Fig. 3D). A possible explanation for this difference is that the conductance of the mGluR6-gated channel is inwardly rectifying, and the lack of inward rectification in control might be due to calcium influx inactivating the channels during the rising phase of the light response. Such an effect would become more pronounced at more negative potentials as the driving force on calcium becomes larger, and is also consistent with the observation that the peak current became larger when BAPTA diffused into the cell (Fig. 3A). In other cases the peak did not increase (Fig. 3B), although this negative result may result from faster run-down of the photoresponse in this cell. If calcium influx

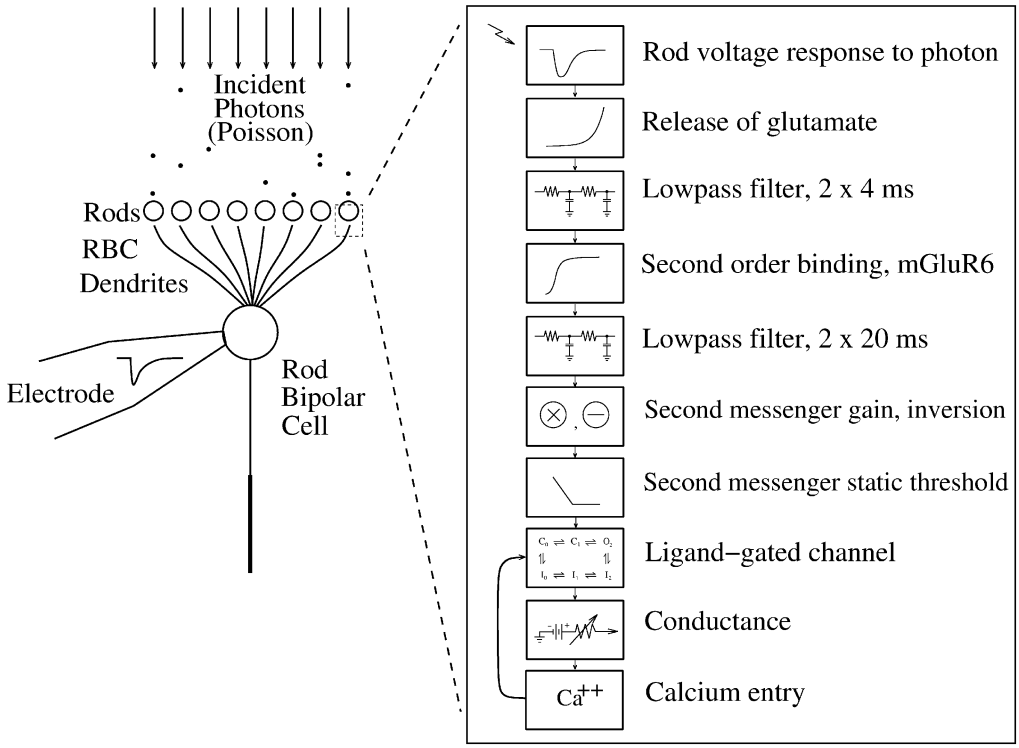

Fig. 9. Outline of the model used to simulate the RBC light responses. The rod membrane potential (top) modulates vesicle release that through a series of mechanisms controls a conductance in the rod bipolar membrane (second from bottom). Calcium (bottom) entering through the channel feeds back to close the channel (third from bottom). The synaptic connections between the rods and the RBC dendrites were isolated, so that calcium influx at a synapse affected only that synapse.

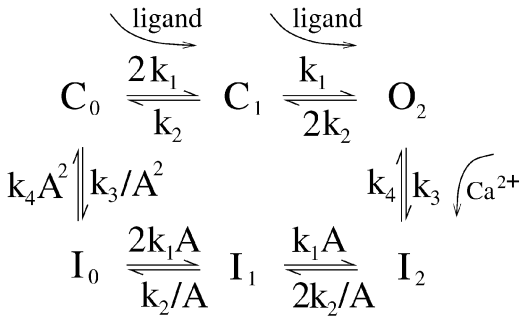

k_1 = binding of ligand
k_2 = unbinding of ligand
k_3 = binding of Ca^{2+}
k_4 = unbinding of Ca^{2+}
$A = 4$

Fig. 10. Kinetic scheme used to model the postsynaptic mGluR6 activated channels in the rod bipolar cell. The values for the rates constants were: $k_1 = 2.7 \times 10^9$ mol$^{-1}\cdot$s^{-1}, $k_2 = 1.35 \times 10^4$ s^{-1}, $k_3 = 3.75 \times 10^6$ mol$^{-1}\cdot$s^{-1} & $k_4 = 0.375$ s^{-1}. The factor A was set to 4. The conductance of O_2 was 650 pS and all other states had zero conductance.

were to suppress the peak current at negative potentials, the average 10–90% rise time of 32 ms ($V_m = -50$ mV, $n = 16$) suggests a rapid effect of calcium on its target.

The Hill coefficient for light steps was lower than for light flashes. This most likely results from calcium feedback. The duration of the step stimuli allows temporal integration to produce larger peak amplitudes for the step responses than the flash responses. However, at higher intensities calcium feedback limits the peak amplitude similarly for both the flash response and the step-response. The result is relatively larger step responses at low intensities, which translate into a lower Hill-coefficient. With intracellular BAPTA there is no calcium feedback to limit high-intensity responses, and the Hill coefficient for steps and flashes are similar (see the Table 1).

A model for calcium action

In the model, as in the mouse retina, the dendrites of each RBC made invaginating contacts with about 20 rods (Tsukamoto et al., 2001). These connections had three basic properties. (1) The signal generated by a single photon in the rod saturated the synapse (van Rossum & Smith, 1998; Berntson et al., 2004; Robson & Frishman, 2004). This means that each dendritic tip generates either no signal when no photons are absorbed, or the same signal whether the connected rod absorbs one or more photons. (2) The calcium

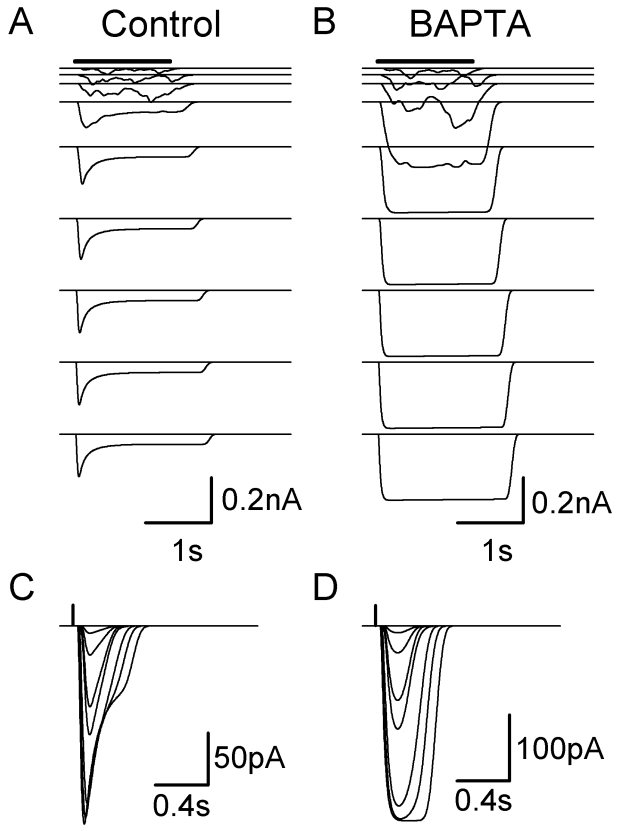

Fig. 11. Step responses and flash responses simulated by the model. The step responses and flash responses in control (*A* & *C*) and with 10 mM intracellular BAPTA (*B* & *D*) compare well with the responses shown in Figs. 4 and 6.

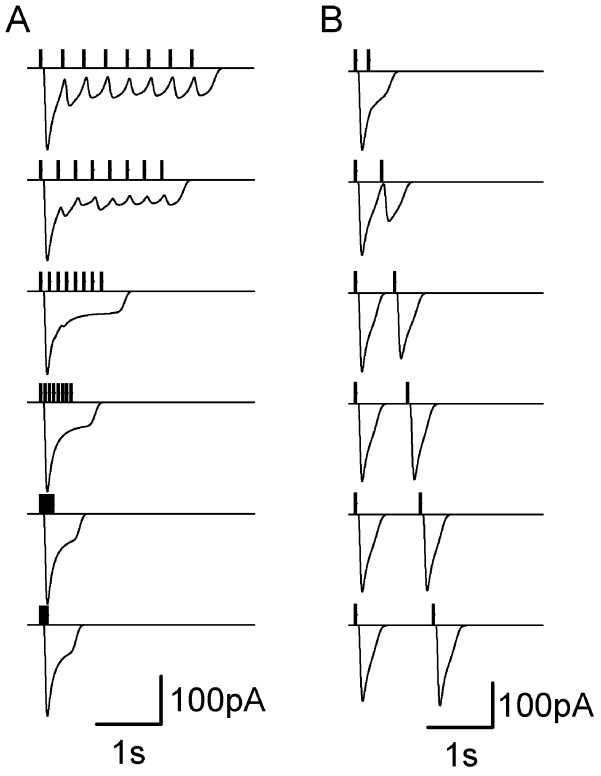

Fig. 12. The model simulations of the flash-train (*A*) and paired-flash experiments (*B*) compare well with the responses shown in Figs. 7 and 8.

influx in one dendritic tip does not affect neighboring dendritic tips, because otherwise inactivation would be observed down to the lowest intensities due to spatio-temporal integration. (3) The influx of calcium during a photoresponse "inactivates" that synapse for about 375 ms. Onset of the inactivation process is evident from the curtailed flash responses in control relative to recordings with intracellular BAPTA. Inactivation causes a strong reduction in synaptic gain, since the postsynaptic response per photon is much smaller. In the model, calcium acts to close the fully liganded channel. This site of action is purely speculative but has been suggested by recent recordings in salamander bipolar cells (Nawy, 2004). The calcium may also interfere with other steps connecting the mGluR6 receptors to the channels. It is interesting to note that although cone bipolar cells also signal *via* mGluR6 receptors, a similar feedback has not been reported, suggesting that there are molecular differences in the two signaling pathways.

According to this model, a low-intensity light step, which delivers photons at Poisson distributed intervals, will most likely activate "naïve" rod synapses (synapses that have not seen a photon for >375 ms) that are in the high gain state (upper 4 records in Figs. 4A & 11A). The resulting signal is maintained for the duration of the step, and displays noise due to stochastic photon capture. At higher light step intensities, the initial transient peak at the onset of the stimulus results from synchronous activation of many of the rod inputs, which are all in the high-gain state. The transient peak current follows the time course of a flash response and is thus independent of the flash intensity (Fig. 5B). A steady plateau current follows the peak current and results from activation of synapses in the low-gain state, where the channels equilibrate between the fully liganded conducting state, O_2, and the fully liganded nonconducting state, I_2 (Fig. 10). The current variance associated with this sustained current is much lower than observed at low intensities, because the photons are arriving at a high enough rate to continuously saturate the synapse and maintain a very low glutamate concentration in the synaptic cleft. The identity of the agonist that opens the light-gated channels in On-bipolar cells is not known, and therefore the agonist has not been explicitly identified in the model. In goldfish and dogfish, evidence indicates that the light-gated channels are cyclic nucleotide gated (Shiells & Falk, 1990, 1992*a*; Henry et al., 2003), but this is not supported by results obtained in salamander (Nawy, 1999).

The role of calcium feedback

Calcium feedback could improve the fidelity of single-photon signal transmission. As noted above, the RBC collects signals from ~20 rods, and in turn it transmits rod signals to the AII amacrine cell with a convergence of ~25:1 (Sterling et al., 1988; Strettoi et al., 1990, 1992). The rod → RBC synapse processes the single-photon signal to remove dark continuous noise (Baylor et al., 1984; van Rossum & Smith, 1998; Field & Rieke, 2002*a*; Berntson et al., 2004), and the second stage of convergence from the RBC onto the AII requires similar quantal processing (Smith & Vardi, 1995). In addition to the continuous dark noise, single-photon signals in rods display variability in both amplitude and duration (Rieke & Baylor, 1998; Whitlock & Lamb, 1999; Field &

Rieke, 2002*b*) The results described here show that the calcium feedback is fast enough to limit the duration and amplitude of the flash response. This implies that the calcium feedback also limits the duration and amplitude of the single-photon response, since the flash response saturates at intensities which produce ~1 photoisomerization per rod (see Table 1, Robson & Frishman, 1995; Berntson et al., 2004). Thus, calcium feedback may filter the RBC response to single photons, and effectively reduce the variability in both the amplitude and duration of the postsynaptic single-photon events (Baylor et al., 1984; Tamura et al., 1989). Such processing might be necessary for improving the reliability of nonlinear processing of the quantal single-photon signal at the second stage of convergence (Smith & Vardi, 1995; Singer & Diamond, 2003).

Because calcium reduces the gain at the rod to RBC synapse, it may also play a role in adaptation (Nawy, 2000). For flash stimuli, which are short compared to the integration time of single-photon responses, the single-photon events are synchronized, and the RBCs are half-saturated when every second rod captures a photon, and become saturated when each rod absorbs in excess of 1 photon. For longer stimuli, the single-photon events are asynchronous, and the rate at which photons are captured needs to be related to the integration time of the single-photon responses. Since the single-photon integration time in mammalian rods is about 200 ms (Penn & Hagins, 1972; Baylor et al., 1984; Field & Rieke, 2002*a*), then during prolonged stimuli that deliver 2.5 photons/rod/s every second rod will be responding to a photon. Prolonged stimuli that deliver ~5 photons/rod/s will saturate the RBC response, but such low intensities will not invoke adaptation within the rods. A recovery time of 375 ms implies that each rod can capture 2–3 photons/s without significant Ca-dependent inactivation of the synaptic transmission. Thus, the recovery time appears fast enough to remove inactivation at light levels below saturation for the RBC, but slow enough to allow inactivation to reduce the postsynaptic response at higher stimulus levels that would otherwise saturate the RBC response. The effect is to increase the rod bipolar's dynamic range, as reflected in the lower Hill coefficient for the step responses.

References

Barlow, H.B., Levick, W.R. & Yoon, M. (1971). Responses to single quanta of light in retinal ganglion cells of the cat. *Vision Research* (Suppl) **3**, 87–101.

Baylor, D.A., Nunn, B.J. & Schnapf, J.L. (1984). The photocurrent, noise and spectral sensitivity of rods of the monkey *Macaca fascicularis*. *Journal of Physiology* **357**, 575–607.

Berntson, A. & Taylor, W.R. (2000). Response characteristics and receptive field widths of on-bipolar cells in the mouse retina. *Journal of Physiology* (London) **524**, 879–889.

Berntson, A., Smith, R.G. & Taylor, W.R. (2003). Transmission of single photon signals through a binary synapse in the mammalian retina. *Visual Neuroscience* **20**, 621–626.

Bloomfield, S.A. & Dacheux, R.F. (2001). Rod vision: Pathways and processing in the mammalian retina. *Progress in Retinal Eye Research* **20**, 351–384.

Dacheux, R. & Raviola, E. (1986). The rod pathway in the rabbit retina: a depolarizing bipolar and amacrine cell. *Journal of Neuroscience* **6**, 331–345.

DeVries, S. & Baylor, D. (1995). An alternative pathway for signal flow from rod photoreceptors to ganglion cells in mammalian retina. *Proceedings of the National Academy of Sciences of the U.S.A.* **92**, 10658–10662.

Dhingra, A., Lyubarsky, A., Jiang, M., Pugh, E.N., Jr., Birnbaumer, L., Sterling, P. & Vardi, N. (2000). The light response of ON bipolar neurons requires G[alpha]o. *Journal of Neuroscience* **20**, 9053–9058.

Dhingra, A., Jiang, M., Wang, T.L., Lyubarsky, A., Savchenko, A., Bar-Yehuda, T., Sterling, P., Birnbaumer, L. & Vardi, N. (2002). Light response of retinal ON bipolar cells requires a specific splice variant of Galpha(o). *Journal of Neuroscience* **22**, 4878–4884.

Euler, T. & Masland, R.H. (2000). Light-evoked responses of bipolar cells in a mammalian retina. *Journal of Neurophysiology* **83**, 1817–1829.

Field, G.D. & Rieke, F. (2002*a*). Nonlinear signal transfer from mouse rods to bipolar cells and implications for visual sensitivity. *Neuron* **34**, 773–785.

Field, G.D. & Rieke, F. (2002*b*). Mechanisms regulating variability of the single photon responses of mammalian rod photoreceptors. *Neuron* **35**, 733–747.

Hack, I., Frech, M., Dick, O., Peichl, L. & Brandstatter, J.H. (2001). Heterogeneous distribution of AMPA glutamate receptor subunits at the photoreceptor synapses of rodent retina. *European Journal of Neuroscience* **13**, 15–24.

Henry, D., Burke, S., Shishido, E. & Matthews, G. (2003). Retinal bipolar neurons express the cyclic nucleotide-gated channel of cone photoreceptors. *Journal of Neurophysiology* **89**, 754–761.

Kamphuis, W., Dijk, F. & O'Brien, B.J. (2003). Gene expression of AMPA-type glutamate receptor subunits in rod-type ON bipolar cells of rat retina. *European Journal of Neuroscience* **18**, 1085–1092.

Kolb, H. & Nelson, R. (1983). Rod pathways in the retina of the cat. *Vision Research* **23**, 301–312.

Kuo, C.C. & Bean, B.P. (1994). Na+ channels must deactivate to recover from inactivation. *Neuron* **12**, 819–829.

Mastronarde, D.N. (1983). Correlated firing of cat retinal ganglion cells. II. Responses of X- and Y-cells to single quantal events. *Journal of Neurophysiology* **49**, 325–349.

Masu, M., Iwakabe, H., Tagawa, Y., Miyoshi, T., Yamashita, M., Fukuda, Y., Sasaki, H., Hiroi, K., Nakamura, Y., Shigemoto, R. al e (1995). Specific deficit of the ON response in visual transmission by targeted disruption of the mGluR6 gene. *Cell* **80**, 757–765.

Nawy, S. (1999). The metabotropic receptor mGluR6 may signal through G(o), but not phosphodiesterase, in retinal bipolar cells. *Journal of Neuroscience* **19**, 2938–2944.

Nawy, S. (2000). Regulation of the on bipolar cell mGluR6 pathway by Ca^{2+}. *Journal of Neuroscience* **20**, 4471–4479.

Nawy, S.A. (2004). Desensitization of the mGluR6 transduction current in tiger salamander on bipolar cells. *Journal of Physiology* **558**, 137–146.

Nawy, S. & Jahr, C.E. (1990). Suppression by glutamate of cGMP-activated conductance in retinal bipolar cells. *Nature* **346**, 269–271.

Nelson, R. (1977). Cat cones have rod input: a comparison of the response properties of cones and horizontal cell bodies in the retina of the cat. *Journal of Comparative Neurology* **172**, 109–135.

Nikonov, S., Engheta, N. & Pugh, E.N., Jr. (1998). Kinetics of recovery of the dark-adapted salamander rod photoresponse. *Journal of General Physiology* **111**, 7–37.

Penn, R. & Hagins, W. (1972). Kinetics of the photocurrent of retinal rods. *Biophysical Journal* **12**, 1073–1094.

Rieke, F. & Baylor, D.A. (1998). Origin of reproducibility in the responses of retinal rods to single photons. *Biophysical Journal* **75**, 1836–1857.

Robson, J.G. & Frishman, L.J. (1995). Response linearity and kinetics of the cat retina: The bipolar cell component of the dark-adapted electroretinogram. *Visual Neuroscience* **12**, 837–850.

Robson, J.G., Maeda, H., Saszik, S. & Frishman, L.J. (2004). *In vivo* studies of signaling in rod pathways using the electroretinogram. *Vision Research* 44, 3253–3268.

Schneeweis, D. & Schnapf, J. (1995). Photovoltage of rods and cones in the macaque retina. *Science* **268**, 1053–1056.

Sharpe, L.T. & Stockman, A. (1999). Rod pathways: the importance of seeing nothing. *Trends in Neuroscience* **22**, 497–504.

Shiells, R.A. & Falk, G. (1990). Glutamate receptors of rod bipolar cells are linked to a cyclic GMP cascade via a G-protein. *Proceedings of the Royal Society B* (London) **242**, 91–94.

Shiells, R.A. & Falk, G. (1992*a*). Properties of the cGMP-activated channel of retinal on-bipolar cells. *Proceedings of the Royal Society B* (London) **247**, 21–25.

Shiells, R.A. & Falk, G. (1992*b*). The glutamate-receptor linked cGMP cascade of retinal on-bipolar cells is pertussis and cholera toxin-sensitive. *Proceedings of the Royal Society B* (London) **247**, 17–20.

Shiells, R.A. & Falk, G. (1994). Responses of rod bipolar cells isolated from dogfish retinal slices to concentration-jumps of glutamate. *Visual Neuroscience* **11**, 1175–1183.

Shiells, R.A. & Falk, G. (1999). A rise in intracellular Ca2+ underlies light adaptation in dogfish retinal 'on' bipolar cells. *Journal of Physiology* (London) **514** (Pt. 2), 343–350.

Shiells, R.A. & Falk, G. (2000). Activation of Ca^{2+}–calmodulin kinase II induces desensitization by background light in dogfish retinal 'on' bipolar cells. *Journal of Physiology* **528**, 327–338.

Singer, J. & Diamond, J.S. (2003). Sustained Ca^{2+} entry elicits transient postsynaptic currents at a retinal ribbon synapse. *Journal of Neuroscience* **23**, 10923–10933.

Slaughter, M.M. & Miller, R.F. (1981). 2-amino-4-phosphonobutyric acid: a new pharmacological tool for retina research. *Science* **211**, 182–185.

Smith, R. & Vardi, N. (1995). Simulation of the AII amacrine cell of mammalian retina: functional consequences of electrical coupling and regenerative membrane properties. *Visual Neuroscience* **12**, 851–860.

Smith, R.G. (1992). NeuronC: A computational language for investigating functional architecture of neural circuits. *Journal of Neuroscience Methods* **43**, 83–108.

Smith, R.G., Freed, M.A. & Sterling, P. (1986). Microcircuitry of the dark-adapted cat retina: Functional architecture of the rod-cone network. *Journal of Neuroscience* **6**, 3505–3517.

Snellman, J. & Nawy, S. (2002). Regulation of the retinal bipolar cell mGluR6 pathway by calcineurin. *Journal of Neurophysiology* **88**, 1088–1096.

Soucy, E., Wang, Y., Nirenberg, S., Nathans, J. & Meister, M. (1998). A novel signaling pathway from rod photoreceptors to ganglion cells in mammalian retina. *Neuron* **21**, 481–493.

Sterling, P., Freed, M.A. & Smith, R.G. (1988). Architecture of rod and cone circuits to the on-beta ganglion cell. *Journal of Neuroscience* **8**, 623–642.

Strettoi, E., Dacheux, R. & Raviola, E. (1990). Synaptic connections of rod bipolar cells in the inner plexiform layer of the rabbit retina. *Journal of Comparative Neurology* **295**, 449–466.

Strettoi, E., Raviola, E. & Dacheux, R.F. (1992). Synaptic connections of the narrow-field, bistratified rod amacrine cell (AII) in the rabbit retina. *Journal of Comparative Neurology* **325**, 152–168.

Tamura, T., Nakatani, K. & Yau, K.W. (1989). Light adaptation in cat retinal rods. *Science* **245**, 755–758.

Tsukamoto, Y., Morigiwa, K., Ueda, M. & Sterling, P. (2001). Microcircuits for night vision in mouse retina. *Journal of Neuroscience* **21**, 8616–8623.

van Rossum, M.C. & Smith, R.G. (1998). Noise removal at the rod synapse of mammalian retina. *Visual Neuroscience* **15**, 809–821.

Vaney, D.I., Young, H.M. & Gynther, I.C. (1991). The rod circuit of the rabbit retina. *Visual Neuroscience* **7**, 141–154.

Vardi, N. (1998). Alpha subunit of Go localizes in the dendritic tips of ON bipolar cells. *Journal of Comparative Neurology* **395**, 43–52.

Vardi, N., Duvoisin, R., Wu, G. & Sterling, P. (2000). Localization of mGluR6 to dendrites of ON bipolar cells in primate retina. *Journal of Comparative Neurology* **423**, 402–412.

Wässle, H., Yamashita, M., Greferath, U., Grünert, U. & Müller, F. (1991). The rod bipolar cell of the mammalian retina. *Visual Neuroscience* **7**, 99–112.

Whitlock, G.G. & Lamb, T.D. (1999). Variability in the time course of single photon responses from toad rods: Termination of rhodopsin's activity. *Neuron* **23**, 337–351.

Wilson, M., Tessier-Lavigne, M. & Attwell, D. (1987). Noise analysis predicts at least four states for channels closed by glutamate. *Biophysical Journal* **52**, 955–960.

Yamashita, M. & Wässle, H. (1991). Responses of rod bipolar cells isolated from the rat retina to the glutamate agonist 2-amino-4-phosphonobutyric acid (APB). *Journal of Neuroscience* **11**, 2372–2382.